REPORT DOCUMENTATION PAGE

Form Approved
OMB No. 0704-01-0188

1. REPORT DATE (DD-MM-YYYY)	2. REPORT TYPE	3. DATES COVERED (From - To)
09-28-2004	REPRINT	

4. TITLE AND SUBTITLE
Reaction Kinetics of PO_2Cl^-, $PO_2Cl_2^-$, $POCl_2^-$, and $POCl_3^-$ Ions with O_2 and O_3 from 163 to 400 K

5a. CONTRACT NUMBER

5b. GRANT NUMBER

5c. PROGRAM ELEMENT NUMBER
62601F

6. AUTHORS
Abel I. Fernandez, Anthony J. Midey*, Thomas M. Miller*, and A.A. Viggiano

5d. PROJECT NUMBER
1010

5e. TASK NUMBER
BM

5f. WORK UNIT NUMBER
A1

7. PERFORMING ORGANIZATION NAME(S) AND ADDRESS(ES)
Air Force Research Laboratory /VSBXT
29 Randolph Road
Hanscom AFB, MA 01731-3010

8. PERFORMING ORGANIZATION REPORT NUMBER
AFRL-VS-HA-TR-2005-1194

9. SPONSORING/MONITORING AGENCY NAME(S) AND ADDRESS(ES)

10. SPONSOR/MONITOR'S ACRONYM(S)
AFRL/VSBXT

11. SPONSOR/MONITOR'S REPORT NUMBER(S)

12. DISTRIBUTION/AVAILABILITY STATEMENT
Approved for public release; distribution unlimited.

13. SUPPLEMENTARY NOTES

14. ABSTRACT Rate constants and product branching ratios for the gas-phase reactions of O_2 and O_3 with the anions (a) PO_2Cl^-, (b) $POCl_3^-$ (c) $POCl_2^-$, and (d) $PO_2Cl_2^-$ were measured in a selected ion flow tube. The kinetics were measured at temperatures of 163-400 K and a He pressure of 0.4 Torr. Only PO_2Cl^- reacts with O_2 to a measureable extent, having $k(163\text{-}400\text{ K}) = 1.1 \times 10^{-8}(T/K)^{-1.0}$ cm^3 molecule^{-1} s^{-1}, while O_3 reacts with all of the anions except $PO_2Cl_2^-$. The fitted rate constant expressions for the O_3 reaction with anions a-c are as follows: $k_a (163\text{-}400\text{ K}) = 3.5 \times 10^{-6} (T/K)^{-1.6}$, $k_b (163\text{-}400\text{ K}) = 4.0 \times 10^{-7} (T/K)^{-1.2}$, and $k_c (163\text{-}400 \text{ k}) = 3.7 \times 10^{-7} (T/K)^{-1.4}$ cm^3 molecule^{-1} s^{-1}. Calculations were performed at the G3 level of theory to obtain optimized geometries, energies, and electron affinities (EAs) of the reactant and product species, as well as to determine the reaction thermochemistry to help understand the experimental results. The PO_xCl_y anions that have lower electron binding energies (cBE) and higher spin multiplicities are more reactive. The doublets are more labile than the singlets. How the extra electron density is distributed in the anion does not predict the observed reactivity of the ion. The reactions of PO_2Cl^- with O_2 and O_3 yield predominantly PO_3^- and PO_4^-. The reaction of $POCl_2^-$ with O_3 yields mostly $PO_2Cl_2^-$, while the $POCl_3^-$ reaction with O_3 yields mostly O_3^- and $PO_2Cl_2^-$.

15. SUBJECT TERMS
Phosphorus oxychlorides
Ozone
Rate constants
Temperature dependences

16. SECURITY CLASSIFICATION OF:

a. REPORT	b. ABSTRACT	c. THIS PAGE	17. LIMITATION OF ABSTRACT	18. NUMBER OF PAGES	19a. NAME OF RESPONSIBLE PERSON
UNCL	UNCL	UNCL	UNL		A. A. Viggiano

19B. TELEPHONE NUMBER (Include area code)
(781) 377-4028

Reaction Kinetics of PO_2Cl^-, $PO_2Cl_2^-$, $POCl_2^-$, and $POCl_3^-$ with O_2 and O_3 from 163 to 400 K

Abel I. Fernandez,[†] Anthony J. Midey, Thomas M. Miller, and A. A. Viggiano*

Air Force Research Laboratory, Space Vehicles Directorate, 29 Randolph Road, Hanscom AFB, Massachusetts 01731-3010

Received: June 7, 2004; In Final Form: August 12, 2004

Rate constants and product ion branching fractions for the gas-phase reactions of O_2 and O_3 with the anions (a) PO_2Cl^-, (b) $POCl_3^-$, (c) $POCl_2^-$, and (d) $PO_2Cl_2^-$ were measured in a selected-ion flow tube (SIFT). The kinetics were measured at temperatures of 163−400 K and a He pressure of 0.4 Torr. Only PO_2Cl^- reacts with O_2 to a measurable extent, having $k(163-400 \text{ K}) = 1.1 \times 10^{-8}(T/\text{K})^{-1.0}$ cm^3 molecule^{-1} s^{-1}, while O_3 reacts with all of the anions except $PO_2Cl_2^-$. The fitted rate constant expressions for the O_3 reaction with anions a−c are as follows: $k_a(163-400 \text{ K}) = 3.5 \times 10^{-6}(T/\text{K})^{-1.6}$, $k_b(163-400 \text{ K}) = 4.0 \times 10^{-7}(T/\text{K})^{-1.2}$, and $k_c(163-400 \text{ K}) = 3.7 \times 10^{-7}(T/\text{K})^{-1.4}$ cm^3 molecule^{-1} s^{-1}. Calculations were performed at the G3 level of theory to obtain optimized geometries, energies, and electron affinities (EAs) of the reactant and product species, as well as to determine the reaction thermochemistry to help understand the experimental results. The $PO_xCl_y^-$ anions that have lower electron binding energies (eBE) and higher spin multiplicities are more reactive. The doublets are more labile than the singlets. How the extra electron density is distributed in the anion does not predict the observed reactivity of the ion. The reactions of PO_2Cl^- with O_2 and O_3 yield predominantly PO_3^- and PO_4^-. The reaction of $POCl_2^-$ with O_3 yields mostly Cl^- and $PO_2Cl_2^-$, while the $POCl_3^-$ reaction with O_3 yields mostly O_3^- and $PO_2Cl_2^-$.

Introduction

The toxicity, reactivity, and decomposition pathways of phosphorus-containing compounds are particularly interesting for their role in the use, production, incineration, and accidental emissions of chemical warfare nerve agents, pesticides, plasticizers, flame retardants, and hydraulic fluids.[1−6] Concerns arise in the contamination of plasma by these compounds in coal-fired magnetohydrodynamic electric generators.[7] Also, flame tests intimate that the addition of a few percent of either phosphine (PH_3) or oxyphosphorus compounds to hydrogen-fueled scramjet combustors yields a measurable increase of the flameholding stability and output thrust in the supersonic expansion because of enhanced H, O, and OH recombination kinetics.[8−12] Furthermore, evidence suggests that combustion is sensitive to and can be enhanced by ion−molecule chemistry.[13] Consequently, the reactions of certain neutral and anionic phosphorus-containing compounds with common gases have been studied,[14−18] in part to elucidate pathways for PO_3^- production.[18,19]

To address these issues, kinetics measurements for the reactions of PO_2Cl^-, $PO_2Cl_2^-$, $POCl_2^-$, and $POCl_3^-$ anions with the oxidants O_2 and O_3 (ozone) have been made. Ozone is interesting because it can attach electrons and it is a very strong oxidant, while reactions with group V compounds producing species such as PO_2 can be chemiluminescent.[20−22] Rate constants and product branching fractions have been measured from 163 to 400 K for the $PO_xCl_y^-$ ions mentioned above and these data are compared with previous work on these systems. However, a dearth of studies of the ion chemistry of these systems exists.[16,23−25] The results of calculations at the G3 level

of theory to obtain optimized geometries, 0 K total energies, 298 K enthalpies, and electron affinities (EA) are also included for the relevant reactant and product molecules. These results have been utilized to determine the reaction thermochemistry and to help understand the experimental data.

Experimental Section

The AFRL selected ion flow tube (SIFT)[26,27] was used to make the measurements. The instrument has been discussed in detail elsewhere and is only briefly described as it pertains to the current experiments. The ions were formed in a remote moderate pressure electron impact ion source at about 0.1 to 1 Torr. PO_2Cl^-, $PO_2Cl_2^-$, $POCl_2^-$, and $POCl_3^-$ were formed from $POCl_3$ (Aldrich, 99%). The $POCl_3$ was used as obtained from the manufacturer except for performing several freeze−pump−thaw steps to remove condensables. Reactant ions were selected with a quadrupole mass filter and then injected into a fast flow of helium buffer gas (AGA, 99.997%) in a 1-m long flow tube using a Venturi inlet, giving a flow tube pressure of 0.4 Torr. The He buffer gas was passed through a liquid nitrogen cooled sieve trap in order to remove water vapor before entering the flow tube. The reactant ions were then thermally equilibrated and proceeded downstream past an inlet used to introduce the neutral reactant. Both O_2 (Massachusetts Oxygen, 99.999%) and O_3 were used alternately in this study. The ozone was produced by interfacing an Orec O3V-0 ozonator to the SIFT apparatus as described in detail in a previous work.[14] This technique yielded a reactant flow of ca. 5% O_3 in O_2. At the end of the reaction tube, a portion of the gas was sampled through an aperture in a blunt nose cone into a second quadrupole, and the mass-filtered ions were counted using a particle multiplier.

The rate constants were obtained from the pseudo-first-order attenuation of the reactant ion signal that depends on the reaction

---

* Corresponding author. E-mail: albert.viggiano@hanscom.af.mil.
[†] National Academy of Sciences Postdoctoral Research Fellow.

Reaction Kinetics of P Compounds with O_2 and O_3

J. Phys. Chem. A, Vol. 108, No. 42, 2004 **9121**

TABLE 1: G3[a] Total Energies, Enthalpies, and Electron Affinities (EA), All Units except EA in Hartrees

species	total energy (0 K)	enthalpy (298 K)	EA[b] (eV)	calcd EA[c] (eV)
$O(^3P)$	−75.03099	−75.02863	1.338 (1.461)[d]	
$O^-(^2P)$	−75.08014	−75.07778		
$O_2(^3\Sigma_g^-)$	−150.24821	−150.24490	0.401 (0.451)[e]	
$O_2^-(^2\Pi_{gi})$	−150.26294	−150.25963		
$O_3(C_{2v},{}^1A_1)$	−225.31826	−225.31437	2.157 (2.1028)[f]	
$O_3^-(C_{2v},{}^2B_1)$	−225.39754	−225.39357		
$Cl(^2P)$	−459.99096	−459.98860	3.609 (3.6127)[g]	
$Cl^-(^1S)$	−460.12360	−460.12124		
$Cl_2(^1\Sigma_g^+)$	−920.07127	−920.06777	2.465 (2.38)[f]	
$Cl_2^-(^2\Sigma_u^+)$	−920.16188	−920.15805		
$ClO(^2\Pi_i)$	−535.12026	−535.11685	2.321 (2.276)[h]	
$ClO^-(^1\Sigma)$	−535.20556	−535.20200		
$ClO_2(C_{2v},{}^2B_1)$	−610.24282	−610.23871	2.245 (2.140)[h]	
$ClO_2^-(C_{2v},{}^1A_1)$	−610.32562	−610.32123		
$Cl_2O(C_{2v},{}^1A_1)$	−995.16647	−995.16208	2.37 (>2.2)[i]	
$Cl_2O^-(C_s,{}^2A')^j$	−995.25362	−995.24808		
$PO_2(C_{2v},{}^2A_1)$	−491.59301	−491.58890	3.464 (3.42,[k] 3.7,[l] 3.6)[m]	
$PO_2^-(C_{2v},{}^1A')$	−491.72030	−491.71624		
$PO_3(C_{2v},{}^2B_2)$	−566.77102	−566.77622	5.155 (4.95)[n]	
$PO_3^-(D_{3h},{}^1A_1)$	−566.96044	−566.95590		
$PO_4(C_{2v},{}^2A_2)$	−641.884035	−641.878008	5.067[o]	
$PO_4^-(C_{2v},{}^1A_1)$	−642.070234	−642.064763		
$POCl_2(C_s,{}^2A')$	−1336.5486	−1336.5429	3.732 (3.8)[p]	3.71
$POCl_2^-(C_s,{}^1A')$	−1336.6857	−1336.6795		
$POCl_3(C_{3v},{}^1A_1)$	−1796.67736	−1796.67057	1.586 (1.4)[p]	1.50
$POCl_3^-(C_s,{}^2A')$	−1796.73562	−1796.72744		
$PO_2Cl(C_{2v},{}^1A_1)$	−951.710965	−951.705948	2.145	
$PO_2Cl^-(C_s,{}^2A')$	−951.789794	−951.784401		
$PO_2Cl_2(C_1,{}^2A)$	−1411.72046	−1411.71449	5.788	
$PO_2Cl_2^-(C_{2v},{}^1A_1)$	−1411.93316	−1411.92673		
$PO_3Cl(C_s,{}^1A)$	−1026.81474	−1026.80895	4.399	
$PO_3Cl^-(C_s,{}^2A)$	−1026.97642	−1026.97046		

[a] The Gaussian 2003 program package[30] was used to perform the calculations. [b] The numbers in parentheses are experimental results from previous work. [c] Calculated EA using the G2 method.[47] [d] Neumark and Lykke.[48] [e] Travers et al.[49] [f] Drzaic et al.[50] [g] Berzinsh et al.[51] [h] Gilles et al.[52] [i] Wecker et al.[53] [j] The structure of this ion (see Table 2) indicates a long Cl–O bond that indicates a more electrostatic interaction which may introduce inaccuracies in the Hartree–Fock zero point energy (ZPE) value since electron correlation is not taken into account. To correct for this, an MP2 calculation was performed and the ZPE was found to be 28 meV greater. Thus, a more accurate estimate of the EA would be lower by this value. [k] Xu et al.[54] [l] Miller.[55] [m] Lohr.[22] [n] Wang and Wang.[19] [o] EA(PO_4) was calculated using the G3B3 method (see text). [p] Mathur et al.[23]

TABLE 2: Bond Lengths (in Å) and Angles (in deg) for Relevant Species Obtained at the G3 Level of Theory, Where the Superscripts Distinguish the O and Cl Atoms

parameter	PO_2Cl^-	$PO_2Cl_2^-$	PO_2Cl_2	PO_2Cl	PO_4^-	PO_3Cl	PO_3^-	Cl_2O^-
$r(P-O)$	1.509	1.491	1.630	1.477	1.666[a]	1.470[b]	1.508	
$r(P-O^2)$			1.477		1.666	1.620		
$r(P-O^3)$					1.496	1.620		
$r(P-Cl^1)$	2.270	2.115	2.010	1.998		1.987		
$r(Cl^1-O)$								1.700
$r(Cl^2-O)$								2.134
$\angle(O^1-P-Cl^1)$	106.28	106.8	98.8	112.7		114.8		
$\angle(O^2-P-Cl^1)$						108.2		
$\angle(O^1-P-O^2)$	125.95	127.5	119.8	134.7[c]	57.7[a]	126.7	120.0	
$\angle(O^2-P-O^3)$					114.6	61.2	120.0	
$\angle(O^3-P-O^4)$					123.2			
$\angle(Cl^1-P-Cl^2)$		98.3		106.9				
$\angle(Cl^1-O-Cl^2)$								116.3
dihed$(O^1,O^2)^d$	136.3		102.0	180.0		147.6		
dihed$(O^1,Cl^2)^e$		110.5						
dihed$(O^1,Cl^1)^f$		127.8	125.7			142.7		
dihed$(O^1,O^3)^f$					104.6			
dihed$(O^1,O^2)^g$					64.1			

[a] PO_4^- has two double bonds and two single bonds. O atoms labeled 1 and 2 are single-bonded while 3 and 4 are double-bonded to P. [b] O atom 1 is double bonded to P while the other two share a bond. [c] The O–P–O angle agrees with the bounded estimate, 130–140°.[45] [d] P–Cl^1 is the reference axis. [e] P–O^1 is the reference axis. [f] P–O^2 is the reference axis. [g] P–O^3 is the reference axis.

to $POCl_2^-$ upon injection into the flow tube was corrected by a similar subtraction procedure because $POCl_2^-$ is also reactive with O_3. Another breakup product is Cl^-; however, a background subtraction could also be used as Cl^- is unreactive with O_2 and O_3.[29] These observations are consistent with previous studies of both dissociative and nondissociative electron attachment to $POCl_3$, where $POCl_2^-$ and Cl^- are the major and minor dissociative products, respectively.[15,16,25] In all cases, the product branching ratios were renormalized after making background corrections.

Computational Method

The Gaussian 03W program package[30] was used to perform calculations on the reactant and product species involved using the G3 theoretical method.[31] The wave function stability of the minimum energy structures from the Hartree–Fock (HF) optimization step of G3 at the 6-31G(d) level have been verified for the neutral and ionic species, with the exception of PO_4 neutral as discussed later. The G3 0 K energies, 298 K enthalpies, and EAs are compared with the literature values whenever possible. These data are given in Table 1 for the optimized structures that have the parameters listed in Table 2. The G3 enthalpies at 298 K have also been used to calculate the heat of reaction at 298 K, ΔH_{rxn}, for all of the pathways discussed in the following sections. The average absolute deviation in the G3 results is ±0.041 eV (0.94 kcal mol^{-1}).[31] Additionally, a natural population analysis[32] (NPA) was used to ascertain the location of the "extra" electron density in the anions; geometries were optimized using MP2(Full) at the 6-311+G(d) level.

Experimental Results

Rate constants and branching fractions for the reactions of PO_2Cl^-, $PO_2Cl_2^-$, $POCl_2^-$, and $POCl_3^-$ with O_2 and O_3 were measured from 163 to 400 K at a He pressure of 0.4 Torr. Only PO_2Cl^- reacts with O_2 to a measurable extent, while $PO_2Cl_2^-$ was found to be unreactive with both O_2 and O_3. This observation is in agreement with earlier work where $PO_2Cl_2^-$, $POCl_2^-$, and $POCl_3^-$ were found to be unreactive with O_2.[17,25]

time and the concentration of the neutral reactant, the latter of which is varied during a measurement. The rate constants have relative uncertainties of ±15% and absolute uncertainties of ±25%.[26] For the product distributions, the SIFT was operated under conditions of modest attenuation of the reactant ion signal and the product branching fractions were extrapolated to a condition of zero neutral reactant concentration. Thus, the effects of secondary chemistry are accounted for. The mass resolution of the downstream mass filter has also been adjusted to minimize mass discrimination during the branching fraction measurements. The branching fractions have relative uncertainties of ±10% of the major product peaks.[28]

Because of the unavoidable presence of O_2 during the O_3 experiments, corrections to the branching fractions for the PO_2Cl^- reaction with O_3 were made by subtracting the product counts from the O_2 reaction with PO_2Cl^-. When the $POCl_3^-$ + O_3 system was studied, the breakup of roughly 5% of $POCl_3^-$
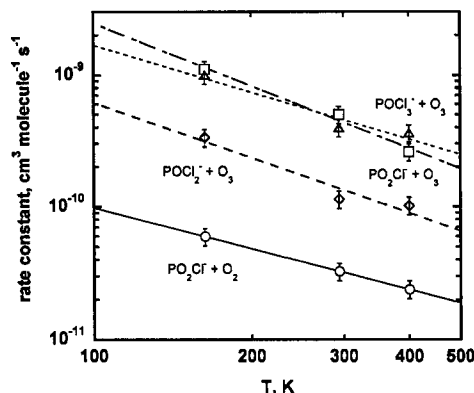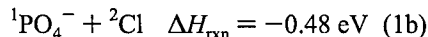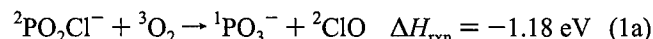
Figure 1. Rate constants in cm^3 s^{-1} for the reactions of PO_2Cl^-, $POCl_2^-$, and $POCl_3^-$ with O_2 and O_3 as a function of temperature in K as measured in a selected ion flow tube (SIFT).

TABLE 3: Rate Constants[a] and Ion Product Branching Fractions for the Reactions of PO_2Cl^-, $PO_2Cl_2^-$, $POCl_2^-$, and $POCl_3^-$ with O_2 and O_3[b]

reaction		163 K	294 K	400 K
$PO_2Cl^- + O_2$		0.60 [6.0]	0.33 [6.0]	0.24[6.0]
→	$PO_3^- + ClO$	0.49	0.42	0.41
	$PO_4^- + Cl$	0.51	0.58	0.59
$PO_2Cl^- + O_3$		11 [9.9]	5.0 [8.9]	2.6 [8.6]
→	$PO_3^- + ClO_2$	0.62	0.65	0.66
	$PO_3^- + Cl + O_2$			
	$PO_4^- + ClO$	0.34	0.34	0.33
	$Cl^- + PO_3 + O_2$	0.04	0.01	0.01
$POCl_2^- + O_3$		3.3 [9.7]	1.1 [8.6]	1.0 [8.3]
→	$Cl^- + PO_2Cl + O_2$	0.71	0.79	0.60
	$Cl^- + PO_3 + ClO$			
	$PO_2Cl_2^- + O_2$	0.26	0.20	0.35
	$PO_3^- + ClO + Cl$	0.02	0.01	0.03
	$PO_3^- + Cl_2O$			
	$PO_4^- + Cl_2$	0.01	≤0.005	0.02
$POCl_3^- + O_3$		10 [9.3]	4.0 [8.3]	3.6 [8.1]
→	$O_3^- + POCl_3$	0.50	0.55	0.55
	$PO_2Cl_2^- + ClO_2$	0.44	0.42	0.44
	$PO_2Cl_2^- + Cl + O_2$			
	$Cl^- + PO_2Cl_2 + O_2$	0.06	0.03	0.01
	$Cl^- + PO_2 + Cl_2 + O_2$			
	$Cl^- + PO_3Cl + ClO$			

[a] Rate constants in units of 10^{-10} cm^3 s^{-1}; bracketed numbers represent calculated collisional rate constants obtained by the parametrized trajectory approach of Su and Chesnavich.[56,57] [b] Measurements of the rate constants of $PO_2Cl_2^-$, $POCl_2^-$, and $POCl_3^-$ with O_2 and of $PO_2Cl_2^-$ with O_3 yielded upper limits of 5×10^{-12} cm^3 s^{-1}.

Moreover, this lack of reactivity is not surprising as the EA of O_2 is smaller than that of $POCl_3$ (see Table 1). The SIFT apparatus is capable of accurate measurement of rate constants approximately as low as 5×10^{-12} cm^3 s^{-1}. Consequently, the rate constants for the reactions of $PO_2Cl_2^-$, $POCl_2^-$, and $POCl_3^-$ with O_2 have a value $<5 \times 10^{-12}$ cm^3 s^{-1}. A similar upper limit can be placed on the rate constant for the reaction of $PO_2Cl_2^-$ with O_3 as it is unreactive as well, since no products are formed.

The rate constants for the reaction of PO_2Cl^- with O_2 given by eq 1

$$^2PO_2Cl^- + {}^3O_2 \rightarrow {}^1PO_3^- + {}^2ClO \quad \Delta H_{rxn} = -1.18 \text{ eV} \quad (1a)$$

$$^1PO_4^- + {}^2Cl \quad \Delta H_{rxn} = -0.48 \text{ eV} \quad (1b)$$

are shown in Figure 1. The superscripts in eq 1 and all subsequent reaction equations denote the spin multiplicity and only the spin-allowed, exothermic channels are given. The energetics of the reactants and products calculated using G3 theory for all the listed reactions are also shown in Table 1. For purposes of efficiency, the rate constant data for all of the reactions studied are shown in Figure 1. A best fit to the rate constants for reaction 1 in Figure 1 yields the expression $k(163-400 \text{ K}) = 1.1 \times 10^{-8}(T/K)^{-1.0}$ cm^3 $molecule^{-1}$ s^{-1}. This case is the only one where oxygen reacts to a measurable extent with $PO_xCl_y^-$ in the SIFT. Clearly, the rate constants decrease with increasing temperature, indicative of a reaction involving either an intermediate collision complex or transfer of an electron.

The product ion branching fractions for the products PO_3^- and PO_4^- are listed in Table 3. The fraction of PO_4^- is somewhat greater than that of PO_3^- at all temperatures and increases with increasing temperature.

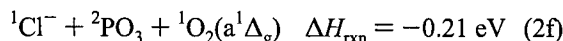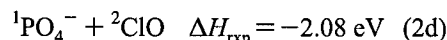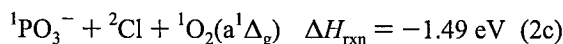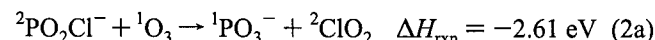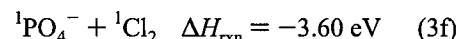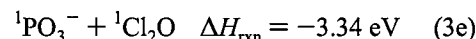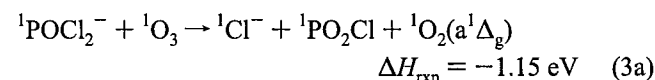The rate constants for the reaction of PO_2Cl^- with O_3 given in eq 2

$$^2PO_2Cl^- + {}^1O_3 \rightarrow {}^1PO_3^- + {}^2ClO_2 \quad \Delta H_{rxn} = -2.61 \text{ eV} \quad (2a)$$

$$^1PO_3^- + {}^2Cl + {}^3O_2 \quad \Delta H_{rxn} = -2.47 \text{ eV} \quad (2b)$$

$$^1PO_3^- + {}^2Cl + {}^1O_2(a^1\Delta_g) \quad \Delta H_{rxn} = -1.49 \text{ eV} \quad (2c)$$

$$^1PO_4^- + {}^2ClO \quad \Delta H_{rxn} = -2.08 \text{ eV} \quad (2d)$$

$$^1Cl^- + {}^2PO_3 + {}^3O_2 \quad \Delta H_{rxn} = -1.19 \text{ eV} \quad (2e)$$

$$^1Cl^- + {}^2PO_3 + {}^1O_2(a^1\Delta_g) \quad \Delta H_{rxn} = -0.21 \text{ eV} \quad (2f)$$

are also shown in Figure 1, while the product branching fractions are listed in Table 3. A best fit to the rate constants gives the expression $k(163-400 \text{ K}) = 3.5 \times 10^{-6}(T/K)^{-1.6}$ cm^3 $molecule^{-1}$ s^{-1} for reaction 2. Clearly, O_3 reacts about an order of magnitude faster than O_2. The same decrease with increasing temperature is also seen with ozone. Unlike the previous reaction, the major product ion is PO_3^- and its fraction is about twice as great than that of PO_4^-. Also, a small amount of Cl^- is produced; however, it is less than 5% of the total products and it also decreases with increasing temperature.

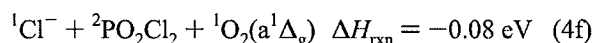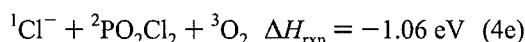The rate constants for the reaction of $POCl_2^-$ with O_3 given by eq 3

$$^1POCl_2^- + {}^1O_3 \rightarrow {}^1Cl^- + {}^1PO_2Cl + {}^1O_2(a^1\Delta_g) \quad \Delta H_{rxn} = -1.15 \text{ eV} \quad (3a)$$

$$^1Cl^- + {}^2PO_3 + {}^2ClO \quad \Delta H_{rxn} = -0.557 \text{ eV} \quad (3b)$$

$$^1PO_2Cl_2^- + {}^1O_2(a^1\Delta_g) \quad \Delta H_{rxn} = -3.86 \text{ eV}^{33} \quad (3c)$$

$$^1PO_3^- + {}^2ClO + {}^2Cl \quad \Delta H_{rxn} = -1.84 \text{ eV} \quad (3d)$$

$$^1PO_3^- + {}^1Cl_2O \quad \Delta H_{rxn} = -3.34 \text{ eV} \quad (3e)$$

$$^1PO_4^- + {}^1Cl_2 \quad \Delta H_{rxn} = -3.60 \text{ eV} \quad (3f)$$

are well fitted by the expression $k(163-400 \text{ K}) = 3.7 \times 10^{-7}(T/K)^{-1.4}$ cm^3 $molecule^{-1}$ s^{-1} and are somewhat less than the rate constants for the PO_2Cl^- reaction. Nevertheless, the rate constants demonstrate the same negative trend with increasing temperature. The product ion branching fractions in Table 3 show that Cl^- is by far the major product, while the $PO_2Cl_2^-$ yield is roughly 25% and increases to 35% at 400 K at the expense of Cl^-. Trace amounts of PO_3^- and PO_4^- were also observed.

TABLE 4: Natural Population Analysis of the PO_xCl_y Species[a]

	charge associated with each atom					
	P	O^1	O^2	Cl^1	Cl^2	Cl^3
$POCl_3$	1.547	−0.95		−0.199	−0.199	−0.199
$POCl_3^-$	1.399	−1.012		−0.404	−0.492	−0.492
extra e⁻	*0.15*	*0.06*		*0.21*	*0.29*	*0.29*
$POCl_2$	1.405	−0.929		−0.238	−0.238	
$POCl_2^-$	1.117	−1.022		−0.547	−0.547	
extra e⁻	*0.29*	*0.09*		*0.31*	*0.31*	
PO_2Cl_2[b]	1.777	−0.435	−0.944	−0.199	−0.199	
$PO_2Cl_2^-$	1.952	−1.063	−1.063	−0.413	−0.413	
extra e⁻	*-0.175*	*0.628*	*0.119*	*0.214*	*0.214*	
PO_2Cl	1.980	−0.883	−0.883	−0.214		
PO_2Cl^-	1.630	−1.048	−1.048	−0.533		
extra e⁻	*0.350*	*0.165*	*0.165*	*0.319*		

[a] Superscripts used to label different O and Cl atoms. [b] Here, the charges on the two O atoms are not equivalent since the P—O bond lengths are not equal; see Table 2.

Finally, the reaction of $POCl_3^-$ with O_3 given by eq 4

$$^2POCl_3^- + {}^1O_3 \rightarrow {}^2O_3^- + {}^1POCl_3 \quad \Delta H_{rxn} = -0.61 \text{ eV} \quad (4a)$$

$$^1PO_2Cl_2^- + {}^2ClO_2 \quad \Delta H_{rxn} = -3.36 \text{ eV} \quad (4b)$$

$$^1PO_2Cl_2^- + {}^2Cl + {}^3O_2 \quad \Delta H_{rxn} = -3.22 \text{ eV} \quad (4c)$$

$$^1PO_2Cl_2^- + {}^2Cl + {}^1O_2(a^1\Delta_g) \quad \Delta H_{rxn} = -2.24 \text{ eV} \quad (4d)$$

$$^1Cl^- + {}^2PO_2Cl_2 + {}^3O_2 \quad \Delta H_{rxn} = -1.06 \text{ eV} \quad (4e)$$

$$^1Cl^- + {}^2PO_2Cl_2 + {}^1O_2(a^1\Delta_g) \quad \Delta H_{rxn} = -0.08 \text{ eV} \quad (4f)$$

$$^1Cl^- + {}^1PO_3Cl + {}^2ClO \quad \Delta H_{rxn} = -0.14 \text{ eV} \quad (4g)$$
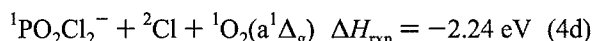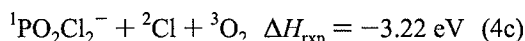
is as rapid as that of PO_2Cl^- with O_3. The best fit expression to the rate constants is $k(163-400 \text{ K}) = 4.0 \times 10^{-7}(T/K)^{-1.2}$ cm³ molecule⁻¹ s⁻¹ for reaction 4. O_3^- is the major product, resulting from direct electron transfer, while the $PO_2Cl_2^-$ product yield is somewhat less. Another similarity with the PO_2Cl^- reaction is the presence of trace amounts of Cl^- product ions which also decrease with increasing temperature.

Computational Results

Table 1 shows the G3 calculated 0 K energies, 298 K enthalpies, and EAs of the relevant species. The calculated EAs and the available experimental values from earlier work are in excellent agreement. The G3(B3LYP) method was used to calculate $EA(PO_4)$ because of a problem in maintaining the lowest-energy wave function throughout the HF and Møller−Plesset (MP) steps of an attempted G3 calculation for neutral PO_4. However, the G3(B3LYP) method is of comparable accuracy to the G3 method.[34]

Table 2 contains the optimized geometries of some of the reactant and product anions. Examining the data in Table 2 shows that the $PO_xCl_y^-$ anions studied in the SIFT all have nonplanar minimum energy structures. PO_2Cl^- and $POCl_2^-$ both have umbrella shaped geometries, while $POCl_3^-$ and PO_3Cl are tetrahedral. Adding the electron to the PO_2Cl neutral shown in Table 2 causes the trigonal planar structure to distort to the umbrella shape. The $PO_2Cl_2^-$ ion has the two O atoms on the same side of the P atom arranged trans to the two Cl atoms on the opposite side.

The results of the NPA computations given in Table 4 show that the electron densities of both the neutral and charged species are concentrated around the more electronegative atoms, Cl and

O. Interestingly, most of the extra electron density from adding an electron to form the anion resides on the Cl atom(s), whereas the O atom(s) receive a much smaller portion. This was also observed in the NPA calculation from the electron attachment study involving $POCl_3$ and PCl_3.[16] The behavior of $PO_2Cl_2^-$ is different than that of the other anions in that the O atoms are not equivalent and do get a considerable portion of the extra density. Moreover, the P atom of PO_2Cl_2 loses electron density upon attachment.

Discussion

It is clear that ozone is more reactive than oxygen, despite the fact that ground-state ozone has a singlet multiplicity while ground-state oxygen is a triplet. These results are consistent with the strong oxidizing ability of ozone.[35] The negative temperature of the rate constants indicates that either a collision complex or a transfer of electrons is involved in the reactions. Ozone reactions with olefins can proceed via channels utilizing five-membered-ring ozonide intermediates.[35,36] If a similar mechanism is involved in these reactions, the ozone could add to the double bond connecting P and O.

Alternatively, a four-membered collision complex may be formed by an O_3 attack on the electropositive P atom of the $PO_xCl_y^-$;[37] the approach would be end-on since the terminal O atoms of O_3 are more negatively charged than the middle atom. The NPA results in Table 4 confirm that the P atom is more positively charged. The more positive middle O atom of O_3 would be attracted to the more negatively charged Cl atoms in the collision complex. The spin-allowed, exothermic product channels are listed in Table 3 and reactions 1−4 may well produce Cl_mO_n neutral fragments or O_2 (a $^1\Delta$), indicating that rearrangements could subsequently occur during the reaction that would result in the observed product ions. A similar mechanism occurs in the reaction of alkyl cations with O_3.[29] In those systems, the intermediate complex forms with the terminal O of O_3 bonded to the positively charged C atom of the ion, followed by rapid O_2 ejection and subsequent rearrangements to give the final products. HF geometry optimizations at the 6-31G(d) level for $PO_xCl_y \cdot O_3^-$ complexes show that stable structures can be found having either the ozonide-type or the alkyl cation−O_3 type structure for PO_2Cl^-, $POCl_2^-$, and $POCl_3^-$. More detailed calculations of the O_3 reaction potential energy surface and detailed reaction paths for the various reactant ions are beyond the scope of this work.

Inspection of Table 4 reveals that there is no correlation between the electron density on the constituent atoms of the $PO_xCl_y^-$ anions and the reactivity. This observation is similar to the computational results of Langeland and Werstiuk regarding the reactivity of several neutral tertiary phosphite esters with O_3. In that work using density functional theory (DFT) and atoms-in-molecules (AIM) methods, no correlation was found between the size of the activation barriers to produce phosphates and $^1O_2$ and the atomic charges on the phosphorus atom or oxygen atoms that make up the four-membered ring of the phosphite ozonide intermediate.[37]

It is interesting to note that only the reaction of $POCl_3^-$ with O_3 undergoes charge transfer. Of the four reactants, only $POCl_3^-$ has an electron binding energy (eBE) that is considerably less than the EA of O_3 (see Table 1). The eBE of PO_2Cl^- is about equal to that of O_3, and the charge-transfer reaction is thermo-neutral but is not observed. Not surprisingly, the more reactive ions, PO_2Cl^- and $POCl_3^-$, have lower eBEs than the less labile $POCl_2^-$. The unreactive $PO_2Cl_2^-$ ion has the highest eBE. A similar observation was made for the $SO_xF_y^-$ species.[38] In

9124 *J. Phys. Chem. A, Vol. 108, No. 42, 2004*

Fernandez et al.

addition, the reactivity can be explained by observing the spin multiplicities of the anion reactants as shown in Table 1 and eqs 1–4. The more reactive ions are doublets, and the less labile species are singlets. Even though examples of fast ion–molecule reactions that do not conserve spin have been observed;[39–42] it is apparent that both the bond strength and spin multiplicity can affect reactivity. Comparable effects of spin multiplicity on reactivity were also observed in an earlier study of $SO_xF_y^-$ reactions with O_3,[43] where another common feature of the $SO_xF_y^-$ and $PO_xCl_y^-$ anions is their lack of reactivity with O_2. Finally, as noted above, there seems to be no correlation between reactivity of the anions and the charges on the constituent atoms.

Conclusions

Rate constants and product branching fractions for the gas-phase reactions of O_2 and O_3 with the anions PO_2Cl^-, $POCl_3^-$, $POCl_2^-$, and $PO_2Cl_2^-$ were measured from 163 to 400 K at 0.4 Torr in a SIFT. Only PO_2Cl^- reacts with O_2 to a measurable extent, while O_3 reacts with all of the ions except $PO_2Cl_2^-$. Stronger reactivity is favored by the following: (a) the weaker bond strength of O_3 relative to O_2, (b) the decreasing eBE of the more reactive anions, and (c) the higher spin-multiplicity of the more reactive anions; i.e., doublets react faster than the singlet species. There is no correlation between reactivity of the anions and electron density of the individual atoms. The reactions of PO_2Cl^- with O_2 and O_3 yield primarily PO_3^- and PO_4^-. The reaction of O_3 with $POCl_2^-$ yields mostly Cl^- and $PO_2Cl_2^-$, while the $POCl_3^-$ reaction with O_3 yields mostly O_3^- and $PO_2Cl_2^-$. G3 calculations were performed to obtain optimized structures, energies, and electron affinities for the reactant and product species and to calculate the thermochemistry for the observed reaction channels. NPA calculations show that the extra electron density added when forming $PO_xCl_y^-$ anions is distributed primarily on the Cl atom(s).

The results presented above could have implications for the technologies mentioned in the Introduction. The metaphosphate anion, PO_3^-, is interesting because it is very stable and it has been detected in combustion environments[44] while the neutral PO_3 radical is associated with phosphorus impurities in coal-fired, magnetohydrodynamic electric generators.[7,19,44] Impurity ions tend to decrease the efficiency of power generation by dilution of the plasma and by radiative loss. The present work shows that the reaction of PO_2Cl^- with O_2 and O_3 yield significant amounts of PO_3^-. However, the ozone is more than an order of magnitude more reactive over the 163–400 K range. This kinetic information may be of use in the modeling of impurity formation in plasmas. PO_2Cl, for example, has a modest EA and can be formed by the reaction of neutral POCl, $POCl_3$, and PCl_3 with O_2.[45]

The PO_2 moiety is thought to be a catalyst in the recombination of H, O, and OH flame species, which can lead to an enhancement of thrust in the supersonic expansion in scramjet exhausts.[8–12] Apparently, the present reactions studied are not capable of directly producing PO_2, as no energetically allowed channels exist. However, reaction 4 has a spin-allowed channel that gives PO_2, but it is endothermic by about 0.5 eV.

It is possible that reactions 1–4 produce the neutral species Cl and ClO, which are known to participate in the catalytic destruction of stratospheric ozone.[46] This potentially negative environmental impact is important when considering the use of oxyphosphorus additives for use in combustion systems.

References and Notes

(1) Corbridge, D. E. C. *Phosphorus An Outline of its Chemistry, Biochemistry, and Technology,* 3rd ed.; Elsevier: Amsterdam, 1980; Vol. 6.

(2) *The Pesticide Manual*; 13th ed.; Tomlin, C., Ed.; British Crop Protection Council: Alton Hampshire, U.K., 2003.

(3) *Handbook of Plasticizers*, 1st ed.; Wypych, G., Ed.; Chem Tec: Toronto, Canada, 2004.

(4) Price, D.; Pyrah, K.; Hull, T. R.; Milnes, G. J.; Ebdon, J. R.; Hunt, B. J.; Joseph, P. *Polym. Degrad. Stab.* **2002**, *77*, 227.

(5) *Handbook of Hydraulic Fluid Power Technology*; Totten, G. E., Ed.; Marcel Dekker: New York, 2000.

(6) Korobeinichev, O. P.; Ilyin, S. B.; Bolshova, T. A.; Shvartsberg, V. M.; Chernov, A. A. *Combust. Flame* **2000**, *121*, 593.

(7) Wormhoudt, J. C.; Kolb, C. E. Mass Spectrometric Determination of Negative and Positive Ion Concentrations in Coal-Fired MHD Plasmas. In *Proceedings of the 10th Materials Research Symposium, Characterization of High-Temperature Vapors and Gases*; Gaithersburg, MD, 1979; U.S. Government Printing Office: Washington, DC, 1979.

(8) Pellett, G. L. *NASA Tech. Rep. 1996* **1996**, 1.

(9) Singh, D. J.; Carpenter, M. H.; Drummond, J. P. *J. Propul. Power* **1997**, *13*, 574.

(10) Twarowski, A. *Combust. Flame* **1993**, *94*, 91.

(11) Twarowski, A. *Combust. Flame* **1995**, *102*, 55.

(12) Mackie, J. C.; Bacskay, G. B.; Haworth, N. L. *J. Phys. Chem. A* **2002**, *106*, 10825.

(13) Williams, S.; Midey, A. J.; Arnold, S. T.; Miller, T. M.; Bench, P. M.; Dressler, R. A.; Chiu, Y.-H.; Levandier, D. J.; Viggiano, A. A.; Morris, R. A.; Berman, M. R.; Maurice, L. Q.; Carter, C. D. Progress on the investigation of the effects of ionization on hydrocarbon/air combustion chemistry: kinetics and thermodynamics of C6–C10 hydrocarbon ions. Presented at the AIAA 4th Weakly Ionized Gases Workshop, Anaheim, CA, 2001.

(14) Williams, S.; Campos, M. F.; Midey, A. J.; Arnold, S. T.; Morris, R. A.; Viggiano, A. A. *J. Phys. Chem. A* **2002**, *106*, 997.

(15) Knighton, W. B.; Miller, T. M.; Grimsrud, E. P.; Viggiano, A. A. *J. Chem. Phys.* **2004**, *120*, 211.

(16) Miller, T. M.; Seeley, J. V.; Knighton, W. B.; Meads, R. F.; Viggiano, A. A.; Morris, R. A.; Van Doren, J. M.; Gu, J.; Schaefer, H. F., III. *J. Chem. Phys.* **1998**, *109*, 578.

(17) Morris, R. A.; Viggiano, A. A. *Int. J. Mass Spectrom. Ion Proc.* **1997**, *164*, 35.

(18) Morris, R. A.; Viggiano, A. A. *J. Chem. Phys.* **1998**, *109*, 4126.

(19) Wang, X.-B.; Wang, L.-S. *Chem. Phys. Lett.* **1999**, *313*, 179.

(20) Toby, S. *Chem. Rev.* **1984**, *84*, 277.

(21) Kampf, R. P.; Parson, J. M. *J. Chem. Phys.* **1998**, *108*, 7595.

(22) Lohr, L. L. *J. Phys. Chem.* **1984**, *88*, 5569.

(23) Mathur, B. P.; Rothe, E. W.; Tang, S. Y.; Reck, G. P. *J. Chem. Phys.* **1976**, *65*, 565.

(24) Goodings, J. M.; Hassanali, C. S. *Int. J. Mass Spectrom. Ion Proc.* **1990**, *101*, 337.

(25) Williamson, D. H.; Mayhew, C. A.; Knighton, W. B.; Grimsrud, E. P. *J. Chem. Phys.* **2000**, *113*, 11035.

(26) Viggiano, A. A.; Morris, R. A.; Dale, F.; Paulson, J. F.; Giles, K.; Smith, D.; Su, T. *J. Chem. Phys.* **1990**, *93*, 1149.

(27) Viggiano, A. A.; Morris, R. A. *J. Phys. Chem.* **1996**, *100*, 19227.

(28) Arnold, S. T.; Williams, S.; Dotan, I.; Midey, A. J.; Morris, R. A.; Viggiano, A. A. *J. Phys. Chem. A* **1999**, *103*, 8421.

(29) Williams, S.; Knighton, W. B.; Midey, A. J.; Viggiano, A. A.; Irle, S.; Morikuma, K. *J. Phys. Chem. A* **2004**, *108*, 1980.

(30) Frisch, M. J.; Trucks, G. W.; Schlegel, H. B.; Scuseria, G. E.; Robb, M. A.; Cheeseman, J. R.; Montgomery, J. A., Jr.; Vreven, T.; Kudin, K. N.; Burant, J. C.; Millam, J. M.; Iyengar, S. S.; Tomasi, J.; Barone, V.; Mennucci, B.; Cossi, M.; Scalmani, G.; Rega, N.; Petersson, G. A.; Nakatsuji, H.; Hada, M.; Ehara, M.; Toyota, K.; Fukuda, R.; Hasegawa, J.; Ishida, M.; Nakajima, T.; Honda, Y.; Kitao, O.; Nakai, H.; Klene, M.; Li, X.; Knox, J. E.; Hratchian, H. P.; Cross, J. B.; Adamo, C.; Jaramillo, J.; Gomperts, R.; Stratmann, R. E.; Yazyev, O.; Austin, A. J.; Cammi, R.; Pomelli, C.; Ochterski, J. W.; Ayala, P. Y.; Morokuma, K.; Voth, G. A.; Salvador, P.; Dannenberg, J. J.; Zakrzewski, V. G.; Dapprich, S.; Daniels, A. D.; Strain, M. C.; Farkas, O.; Malick, D. K.; Rabuck, A. D.; Raghavachari, K.; Foresman, J. B.; Ortiz, J. V.; Cui, Q.; Baboul, A. G.; Clifford, S.; Cioslowski, J.; Stefanov, B. B.; Liu, G.; Liashenko, A.; Piskorz, P.; Komaromi, I.; Martin, R. L.; Fox, D. J.; Keith, T.; Al-Laham, M. A.; Peng, C. Y.; Nanayakkara, A.; Challacombe, M.; Gill, P. M. W.; Johnson,

B.; Chen, W.; Wong, M. W.; Gonzalez, C.; Pople, J. A. *Gaussian 03*, revision B.02. Gaussian, Inc.: Pittsburgh, PA, 2003.

(31) Curtiss, L. A.; Redfern, P. C.; Raghavachari, K.; Rassolov, V.; Pople, J. A. *J. Chem. Phys.* **1998**, *109*, 7764.

(32) Reed, A. E.; Weinstock, R. B.; Weinhold, F. J. *Chem. Phys.* **1985**, *83*, 735.

(33) Huber, K. P.; Herzberg, G. *Molecular Spectra and Molecular Structure. IV. Constants of Diatomic Molecules*; Van Nostrand Reinhold: New York, 1979.

(34) Baboul, A. G.; Curtiss, L. A.; Redfern, P. C.; Raghavachari, K. *J. Chem. Phys.* **1999**, *110*, 7650.

(35) Horvath, M.; Bilitzky, L.; Huttner, J. *Ozone*; Elsevier: Amsterdam, 1985.

(36) Gillies, J. Z.; Gillies, C. W.; Suenram, R. D.; Lovas, F. J. *J. Am. Chem. Soc.* **1988**, *110*, 7991.

(37) Langeland, J. L.; Werstiuk, N. H. *Can. J. Chem.* **2003**, *81*, 525.

(38) Arnold, S. T.; Miller, T. M.; Viggiano, A. A. *J. Phys. Chem. A* **2002**, *106*, 9900.

(39) Fehsenfeld, F. C.; Ferguson, E. E.; Schmeltekopf, A. L. *J. Chem. Phys.* **1966**, *44*, 3022.

(40) Paulson, J. F.; Mosher, R. L.; Dale, F. *J. Chem. Phys.* **1966**, *44*, 3025.

(41) Ferguson, E. E. *Chem. Phys. Lett.* **1983**, *99*, 89.

(42) Federer, W.; Villinger, H.; Lindinger, W.; Ferguson, E. E. *Chem. Phys. Lett.* **1986**, *123*, 12.

(43) Viggiano, A. A.; Arnold, S. T.; Williams, S.; Miller, T. M. *Plasma Chem. Plasma Proc.* **2002**, *22*, 285.

(44) Henchman, M.; Viggiano, A. A.; Paulson, J. F.; Freedman, A.; Wormhoudt, J. *J. Am. Chem. Soc.* **1985**, *107*, 1453.

(45) Ahlrichs, R.; Ehrhardt, C.; Lakenbrink, M.; Schunck, S.; Schnokel, H. *J. Am. Chem. Soc.* **1986**, *108*, 3596.

(46) Molina, M.; Rowland, F. S. *Nature (London)* **1974**, *249*, 810.

(47) Miller, T. M.; Viggiano, A. A.; Morris, R. A.; Miller, A. E. S. *J. Chem. Phys.* **1999**, *111*, 3309.

(48) Neumark, D. M.; Lykke, K. R. *Phys. Rev. A* **1985**, *32*, 1890.

(49) Travers, M. J.; Cowles, D. C.; Ellison, G. B. *Chem. Phys. Lett.* **1989**, *164*, 449.

(50) Drzaic, P. S.; Marks, J.; Brauman, J. I. Electron photodetachment from gas-phase molecular anions. In *Gas-Phase Ion Chemistry: Ions and Light*; Bowers, M. T., Ed.; Academic: New York, 1984; Vol. 3; p 168.

(51) Berzinsh, U.; Gustafsson, M.; Hanstorp, D.; Klinkmueller, A. E.; Ljungblad, U.; Maartensson-Pendrill, A.-M. *Phys. Rev. A* **1995**, *51*, 231.

(52) Gilles, M. K.; Polak, M. L.; Lineberger, W. C. *J. Chem. Phys.* **1992**, *96*, 8012.

(53) Wecker, D.; Christodoulides, A. A.; Schindler, R. N. *Int. J. Mass Spectrom. Ion Phys.* **1981**, *38*, 391.

(54) Xu, C.; de Beer, E.; Neumark, D. M. *J. Chem. Phys.* **1996**, *104*, 2749.

(55) Miller, W. J. *J. Chem. Phys.* **1978**, *69*, 3709.

(56) Su, T.; Chesnavich, W. J. *J. Chem. Phys.* **1982**, *76*, 5183.

(57) Su, T. *J. Chem. Phys.* **1988**, *89*, 5355.